مجلة الدراسات التربوية والعلمية - كلية التربية - الجامعة العراقية
العدد السادس والعشرون - المجلد الأول - علوم الفيزياء - أيلول 2025 م
doi.org/10.52866/esj.2025.01.26.26

Theoretical study of the effect of concentration on the charge transfer rate on N3 dye with zinc sulfide semiconductors

Zainab Amjad Hamid[1] , **Mohsin A. Hassooni**[2*]
Department of Physics ,College of Education for Pure Science Ibn-ALHaitham, University of Baghdad, Baghdad-Iraq
*Corresponding Author. Mohsin A. Hassooni
[a] *E-mail: zainab.amjad2204m@ihcoedu.uobaghdad.edu.iq*
[b] *E-mail:* mohsin.a@ihcoedu.uobaghdad.edu.iq

Abstract :

This study used a theoretical model to study and calculate the electron transfer rate to examine the efficiency of the heterogeneous N3-Zns device using several solvents. This research studied the effect of charge carrier concentration on the donor-to-acceptor electron flow rate of dye-sensitized solar cells. Based on the quantum electron transport theory to describe the N3-ZnS devices, although the transition energy of the system changes with different solvents due to solvation effects (such as changes in dielectric constant and polarization), the charge transfer rate shows different behaviors under various solvents at the same driving force energy value because the system operates in the inverted and normal Marcus regions. The charge transfer rate increased with the increase of charge carrier concentration, temperature, and coupling strength. The highest electron transfer rate was obtained using the morpholine solvent when the charge carrier concentration was N_s=1.4×10^{20} m^{-3} compared to N_s=8.25×10^{17} m^{-3} and for the same solvent.

Keywords: *charge transfer, rate, N3/ZnS, concentration ,Temperature effect.*

دراسة نظرية لتأثير التركيز على معدل انتقال الشحنة على صبغة N3 مع شبة الموصل كبريتيد الزنك

زينب امجد حميد ، محسن عنيد حسوني
قسم الفيزياء، كلية التربية للعلوم الصرفة - ابن الهيثم ، جامعة بغداد، بغداد، العراق

مستخلص:

استخدمت هذه الدراسة نموذجًا نظريًا لدراسة وحساب معدل الانتقال الإلكتروني لتحديد كفاءة النبيطة N3-Zns الغير متجانسة باستعمال العديد من المذيبات. تم دراسة في هذا البحث تأثير تركيز حاملات الشحنة على معدل التدفق الإلكتروني من المانح إلى المستقبل للخلايا الشمسية المتحسسة ذات الصبغة. بناءً على نظرية الانتقال الإلكتروني الكمومي لوصف نبيطة N3-Zns، على الرغم من أن طاقة الانتقال لنظام N3-ZnS تتغير مع اختلاف المذيبات المستخدمة بسبب تأثيرات المذيب (مثل التغيرات في ثابت العزل الكهربائي و الاستقطابية)، إلا أن معدل انتقال الشحنة يظهر سلوكيات مختلفة تحت مذيبات مختلفة عند نفس قيمة طاقة القوة الدافعة لأن النظام يعمل في مناطق ماركوس العكسية والطبيعية. يزداد معدل الانتقال للشحنة مع زيادة تركيز حاملات الشحنة ودرجة الحرارة وقوة الاقتران. تم الحصول على أعلى معدل للانتقال الإلكتروني باستخدام مذيب المورفالين عندما كان تركيز حامل الشحنة N_s=1.4×10^{20} m^{-3} بالمقارنة مع N_s=8.25×10^{17} m^{-3} وللمذيب نفسه.

الكلمات المفتاحيه: انتقال الشحنة، المعدل، N3/ZnS، التركيز، تأثير درجة الحرارة .

1. Introduction

The urgent need to cut greenhouse gas emissions has driven many countries to decrease their dependence on fossil fuels and transition to renewable energy sources. Among the various renewable energy technologies, photovoltaic (PV) technology has gained considerable attention for its ability to directly convert solar energy into high-quality electrical power.[1].

PV cells, or solar cells, have progressed through multiple generations of technology. The first-generation PV cells, which are the most commonly used globally, continue to dominate the commercial market due to their reliability and long lifespan. These cells are typically made from single or multi-crystalline silicon. In contrast, second-generation PV cells utilize thin-film semiconductor materials instead of crystalline silicon. While they tend to be less efficient than first-generation cells, they differ in terms of materials and manufacturing processes.[2]

Dye-sensitized solar cells (DSSCs) have emerged as a promising alternative energy source because of their high efficiency, affordability, ease of manufacture, and environmental friendliness.[3]. Furthermore, DSSC consists of a photosensitive electrode and another electrode that, together with an electrolyte, can convert light energy into electric current[4]. One of the most significant operations that has a significant impact on the DSSC operating systems is the electronic transfer procedure [5] . The process by which dye molecules transport electrons to semiconductor material is the primary determinant of DSSC efficiency[6] .

One of the most basic models for discussing electron transfer is the donor-acceptor model, which does not create or break any chemical bonds inside the system [7]. The researchers developed the electron transfer theory experimentally using spectroscopic and time-resolved techniques, as well as theoretically using analytical approaches and computer simulation [8]. According to quantum framework of electron transfer theory, the greater issue is to pay attention to the touch interface between two materials that require an electron to be transferred from the donor state to the acceptor state [9].

Additionally,as charge transfer occurs at the interface, the interaction

between molecules and semiconductor systems has gained more attention due to its importance in various technological applications [10].

According to Hadi et al., the orientation energy of molecules affects their photophysical properties, including how they interact with light and transfer electrons. The way molecules are oriented influences the alignment of their energy levels, which is crucial for efficient electron transfer. Proper energy level alignment between the donor (such as a dye) and acceptor (such as a semiconductor) is necessary for optimal charge injection and extraction in devices. Therefore, the orientation energy plays a key role in ensuring that energy levels are properly aligned for effective electron transfer in these systems[11].

As charge transfer occurs across the interface, the interaction between molecules and semiconductor systems has gained more attention because of its effect on energy level alignment. The charge transfer process can greatly affect how the energy levels of molecules align with the conduction and valence bands of semiconductors. This alignment is critical because it determines the efficiency of charge injection and extraction, which impacts the performance of devices and solar cells. In many cases, the transfer of electrons can cause shifts in the energy levels, either lowering or raising the work function of the material and these affect on transition energy to reconfiguration. Proper alignment ensures that electrons can flow smoothly across the interface, enhancing the overall device performance and energy conversion efficiency. As a result, charge transfer mechanisms in diverse hetero-structure devices can occur in different photovoltaic devices, influencing their photophysical properties [12].

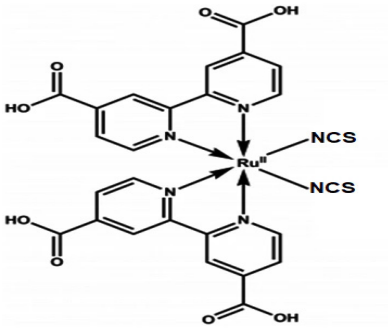

Figure 1: Structure of N3 dye

N3 dye, also known as ruthenium (II)-tris(bipyridyl-2,2'-bis(trifluoromethyl)-4,4'-dicarboxylate), has become a key sensitizer in DSSC research. N3 dye is known for its ex-

cellent light-harvesting properties and efficient electron injection into semiconductors, playing a vital role in improving the overall performance of photovoltaic DSSCs [13]. Its structure is shown in Figure (1) [14].

Understanding the charge transfer between N3 dye and ZnS plays an important role in enhancing the efficiency of dye-sensitized solar cells (DSSCs). N3 dye is widely used in DSSCs for its good light absorption properties and efficient electron injection into ZnS semiconductors. Combined with ZnS, a wide bandgap semiconductor, the charge transfer dynamics become key in improving the performance of DSSCs. The charge transport research in this system sheds light on how the dye's excited state electrons are injected into the ZnS conduction band after absorbing sunlight. The interface between the N3 dye and ZnS affects the efficiency of this electron transfer, as well as the recombination rate of photogenerated charge carriers. The crucial factor is the alignment of the energy levels between the dye and ZnS, which affects the injection efficiency and the extent of charge recombination, and thus the overall performance of the device.

Compared with (Marwa Beital 2018 and Jishad Salam et al. 2025) conducted on DSSCs using TiO2 and ZnO semiconductors, the inclusion of ZnS offers advantages such as high charge transfer and recombination losses, which can improve the overall efficiency of on the other hand, charge transfer studies have shown that the interaction between N3 dye and ZnS requires fine tuning of the interface properties to maximize the charge transfer efficiency. In contrast, other semiconductors such as TiO2 may exhibit more stable long-term performance, although ZnS-based DSSCs may offer higher initial efficiency under ideal conditions [15,16].

The ZnS semiconductor is currently widely employed as a donor electrode in solar cells. Zinc sulfide (ZnS) has special features that make it an attractive choice for optical applications. It is suitable for optical applications because a material's optical property depends on its bandgap, which can be tuned by varying the particle size near the exciton Bohr radius. It also has a wide direct bandgap, 2.5 nm exciton Bohr radius, and exciton binding energy of 39 meV. It is also economical,

environmentally friendly, and chemically stable [17]. This work aimed to theoretically investigate the effect of electron carrier concentration on the electron transport rate in a dye-sensitized solar cell system consisting of N3 dye contacted with zinc sulfide (ZnS) semiconductors. The study addressed the effect of carrier concentration based on the application of quantum electron transfer theory as well as factors such as temperature and coupling strength in influencing the efficiency of the N3-ZnS system in different solvents. In addition, studies examine the transition energy and behavior of charge transfer rates that vary across different solvents, with an emphasis on the effects of concentration on electron flow from donor to acceptor. In this study, we conducted simulations using MATLAB software. Additionally, the computational accuracy of the simulation was deemed acceptable for verifying the results.

2. Theory

The calculation of the electron transfer coefficient in the N3-ZnS system can be done assuming a Hilbert space description of the system. The electron transfer from the N3 donor to the ZnS acceptor is time-dependent and can be treated using perturbation theory methods. The complete wave set for the N3 donor state and the ZnS acceptor state in Hilbert space is given by [18] .

$$|\phi_{N3}\rangle = \sum_i^{\infty} D_i \, |\phi_{N3}(r)\rangle \quad \text{..... (1)}$$

$$|\phi_Z|\phi_{N3}\rangle = \sum_j^{\infty} A_j \, |\phi_{ZnS}(r)\rangle \quad \text{..... (2)}$$

Where $|H\phi_{N3}\rangle$ and $|\phi_{ZnS}\rangle$ are the wave functions for the dye and the semiconductor, respectively. The evolution of the electron transfer coefficient in the semiconductor-dye system can represent the transfer process from the semiconductor to the dye, assuming a Hamiltonian $\hat{H}_S$ consisting of three terms given by [19].

$$\hat{H}_s = \hat{H}_{N3} + \hat{H}_{ZnS} + \hat{H}_{N3/ZnS} \quad \text{..... (3)}$$

where $\hat{H}_{N3}$ is the Hamiltonian operator of N3 dye, $\hat{H}_{ZnS}$ is the Hamiltonian operator of semiconductors and $\hat{H}_{N3/Se}$ is the Hamiltonian operator at the interface of N3-ZnS. [20]

$$\hat{H}_s(|\phi_{N3}\rangle + |\phi_{ZnS}\rangle)e^{\frac{-i}{\hbar}E_n t} = \hat{E}_S(|\phi_{N3}\rangle + |\phi_{ZnS}\rangle)e^{\frac{-i}{\hbar}E_n t} \quad \text{..... (4)}$$

Under non-adiabatic approximation, the electrons satisfy the Schrodinger equation, which describes the state of the electrons interacting in the donor-acceptor system, reads:

$$\hat{\mathbf{E}}_S(|\phi_{N3}\rangle + |\phi_{ZnS}\rangle)e^{\frac{-i}{\hbar}E_n t} = i\hbar\frac{\partial}{\partial t}(|\phi_{N3}\rangle + |\phi_{ZnS}\rangle)e^{\frac{-i}{\hbar}E_n t} \quad (5)$$

$$i\hbar\frac{\partial C_{DA}}{\partial t} = e^{i\frac{E_{ZnS}t}{\hbar}}\left\langle\phi_{ZnS}(r)\left|\hat{H}_{\frac{N3}{ZnS}}\right|\phi_{N3}(r)\right\rangle e^{-i\frac{E_{N3}t}{\hbar}} \quad (6)$$

$$C_{DA} = \frac{1}{i\hbar}\int_0^{\infty}\langle\hat{H}_{\frac{N3}{ZnS}}\rangle e^{-\frac{i}{\hbar}(E_{N3}-E_{ZnS})t}dt \quad (7)$$

The quantity of square magnitude of C_{DA} indicate the probability of density in the form [21]

$$\rho_{DA} = |C_{DA}|^2 \quad \ldots\ldots\ldots\ldots \quad (8)$$

And the probability of density reduced to.

$$\rho_{DA} = \sqrt{\frac{1}{4\pi\Lambda k_B T}}e^{-\frac{(\Lambda+\Delta^0)^2}{4\Lambda k_B T}} \quad \ldots\ldots\ldots\ldots \quad (9)$$

Where Λ is transition energy, k_B is Boltzmann constant, temperature (T) and effective driving energy Δ^0 [22]. For all electrons to give, the possibility of electronic transport has been introduced.

$$\Gamma_{ET} = \frac{2\pi}{\hbar}\sqrt{\frac{1}{4\pi\Lambda k_B T}}\int\left|\langle H_{\frac{Se}{Dye}}(E)\rangle\right|^2 F_{(E)}\, e^{-\frac{(\Lambda+(E_c-qE^o))^2}{4\Lambda k_B T}}\delta(E_{Se}-E_{Dye})dE \quad \ldots\ldots \quad (10)$$

The activation density of state for semiconductor-dye system ϱ_{act} (E) for electronic transport rate is given by [23].

$$\varrho_{act}(E) = \delta(E_{Se}-E_{Dye}) = \rho_S\frac{I_e}{\sqrt[3]{\frac{6d_a^2}{\pi}}} \quad \ldots\ldots\ldots\ldots\ldots\ldots \quad (11)$$

Where ρ_S is the electronic density in the semiconductor, d_a is the atomic density of the semiconductor and I_e is length coupling. The rate of electronic transport is decay with distance by a constant a and given by [24] .

$$\Pi_{et} = \frac{\Gamma_{ET}}{\alpha} \quad \ldots\ldots\ldots\ldots\ldots\ldots \quad (12)$$

Inserting Eq.(11) together (12) in Eq.(13) to given

$$\Pi_{et} = \frac{2\pi}{\hbar}\frac{\left|\langle \hat{H}_{\frac{N3}{ZnS}} \rangle\right|^2}{\alpha}\sqrt{\frac{1}{4\pi\Lambda_{\frac{N3}{ZnS}} k_B T}}\, e^{-\frac{\left(\Lambda_{\frac{N3}{ZnS}}+\Delta^0\right)^2}{4\Lambda_{\frac{N3}{ZnS}} k_B T}}\frac{I_e}{\sqrt[3]{\frac{6d_a^2}{\pi}}}N_s(E) \qquad \text{..... (13)}$$

The transition energy of the solvent circumfluent the system at the new equilibrium of the system is [25].

$$\Lambda_{N3/ZnS}(eV) = \frac{e^2}{8\pi\varepsilon_0}\frac{1}{D_{dye}}\left(\frac{1}{{n_{so}}^2}-\frac{1}{\epsilon_{so}}\right) - \frac{e^2}{8\pi\varepsilon_0}\frac{1}{2R}\left(\frac{n_{Se}^2-{n_{so}}^2}{n_{Se}^2+{n_{so}}^2}\frac{1}{{n_{so}}^2}-\frac{\epsilon_{Se}^2-{\epsilon_{so}}^2}{\epsilon_{Se}^2+\epsilon{\epsilon_{so}}^2}\frac{1}{{\epsilon_{so}}^2}\right) \quad \text{.... (14)}$$

where e is the electron charge, ε_0 is permittivity D and R are the radius of the dye and the distance between the dye and semiconductor, n_{se} and ϵ_{se} are s the refractive index and dielectric constant of the semiconductor, n_{so} and ϵ_{so} are the optical and statistical dielectric constant of solvents.

$$r(m) = \sqrt[3]{\frac{3}{4\pi}\frac{M}{N_A\rho}} \qquad \text{..... (15)}$$

Where M is the molecular weight, N_A is the Avogadro number, and ρ is the mass density .

3. Results and Discussion

The electron transfer rate of a dye-semiconductor interface with different solvents is calculated and evaluated based on the continuum state and quantitative charge transfer model using MATLAB. Depending on the transition energy, which plays a key role in limiting electron transfer, the rate of electron transfer from the excited dye N3 to ZnS can be calculated. The transition energy was calculated using the Eq. (14) depending on the radii of the dye N3, semiconductor ZnS, refractive index, dielectric ZnS, and solvent. The radii of ZnS and N3 depending on Eq.(15) with molecular weight and mass density of N3 from table (1) and molecular weight and mass density for ZnS from table (2) and results radii are R_{N3} =5.9 A° and R_{Zns}= 2.115 (Å) for both N3 and *Zns* respectively .

Table 1: Characteristics of N3 dye molecules [26], [27]

The N3 Molecule dye	
Name of Dye	Cis-bis(isothiocyanato)bis(2,2′-bipyridyl-4,4′-dicarboxylato)ruthenium(II)
Chemical formula	$[C_{26}H_{16}N_6O_8RuS_2]$
Molar Mass	705.64 g/mol
Density	1.36 g/c^{m}3
Melting point	>300C^o
HOMO	-5.39 eV
LUMO	-2.79 eV
Calculated radius	5.9 A^o

Table 2: General properties of ZnS semiconductor *[28], [29]*

Properties	ZnS
Molecular Weight	97.46 g/mol
Group	Zinc – 12
	Sulfur - 16
Crystal Structure	Cubic
Lattice Constant	5.4093 Å
Dielectric Constant	8.9
Band Gap	3.54 eV
Electron Mobility	180 cm^2/Vs
Hole Mobility	5 cm^2/Vs
Density	4.079 g/cm^3
Melting Point	1850°C
Refractive Index	2.356
Radii	2.1158115 (Å)

From the Eq (14), the values of the transition energy $\Lambda_{N3/ZnS}$ were calculated by inserting the refractive index of the semiconductor and the dielectric constant of ZnS from Table (2) and the dielectric constant and refractive index of the solvents used from Table 3. The obtained values of the transition energy are shown in Table (3).

Table 3: Calculated results of transition energy $\Lambda_{N3/ZnS}$ (eV) for N3-ZnS

solvents	Chemical formula	(n)30]]	(ε) [30]	$\Lambda_{N3/ZnS}$ (eV)
Morpholine	$C_4H_9N_1O$	1.4545	7.33	0.3167
Acetic acid	$C_2H_4O_2$	1.3720	6.15	0.3361
1,2-Dim ethoxyethane	$C_4H_{10}O_2$	1.3790	7.2	0.3582
Butanol	$C_4H_{10}O$	1.3970	17.51	0.4441
Propanol-1	C_3H_8O	1.3837	20.33	0.4621
Ethanol	C_2H_6O	1.3610	24.5	0.4871
Propionitrile	C_3H_5N	1.3636	27.20	0.4904
Acetonitrile	C_2H_3N	1.3416	37.50	0.5176
Methanol	CH_4O	1.3280	32.7	0.5222

The Eq.(13) was used to calculate the electronic transfer rate by entering the effective driving energy for N3/ZnS system $\Delta^0 = 0.27$ (eV) , for the temperatures 320 K and 325 K , and using two values carrier concentration N_e=1.4×10^{20} m^{-3} and N_e=8.25×10^{17} m^{-3} m^{-3} [31] , taken the transition energy-for N3/*ZnS* with solvents , coupling strength $\left|\langle H_{\frac{ZnS}{N3}}(E)\rangle\right|^2 = (1\ to\ 4)\ x10^{-3}\ |eV|^2$ [32], effective length l_e=3A^0[33] , atomic density d_{ZnS}=2.52039 $x10^{25}$ 1/m^3 and electronic concentration α=1×10^{10} 1/m with MATLAP program, results list in the Tables from (4) ,(5),(6) and (7) for N3/*ZnS* devices at temperature 320 K, 325 K respectively.

***Table 4: Results of electronic transition flow for** N3- ZnS **devices system at** Δ^0=0.27 (*eV*) *and* N_s=8.25×10^{17} m^{-3} *with* T=320 K .*

solvent	$\Lambda_{\frac{N3}{ZnS}}(eV)$	Rate of Electronic Transfer cm^2/Sec						
		$\langle \hat{H}_{\frac{N3}{ZnS}} \rangle$ eV/ state						
		1×10^{-3}	1.5×10^{-3}	2×10^{-3}	2.5×10^{-3}	3×10^{-3}	3.5×10^{-3}	4×10^{-3}
Morpholine	0.3167	3.5427E-10	5.3141E-10	7.0854E-10	8.8568E-10	1.0628E-09	1.2400E-09	1.4171E-09
Acetic acid	0.3361	3.2524E-10	4.8787E-10	6.5049E-10	8.1311E-10	9.7573E-10	1.1384E-09	1.3010E-09
1,2-Dim ethoxyethane	0.3582	2.9115E-10	4.3672E-10	5.8229E-10	7.2786E-10	8.7344E-10	1.0190E-09	1.1646E-09
Butanol	0.4441	1.7151E-10	2.5727E-10	3.4302E-10	4.2878E-10	5.1454E-10	6.0029E-10	6.8605E-10
Propanol-1	0.4621	1.5134E-10	2.2702E-10	3.0269E-10	3.7836E-10	4.5403E-10	5.2970E-10	6.0537E-10
Ethanol	0.4871	1.2654E-10	1.8981E-10	2.5308E-10	3.1635E-10	3.7962E-10	4.4289E-10	5.0616E-10
Propionitrile	0.4904	1.2350E-10	1.8525E-10	2.4700E-10	3.0875E-10	3.7050E-10	4.3225E-10	4.9400E-10
Acetonitrile	0.5176	1.0084E-10	1.5126E-10	2.0168E-10	2.5209E-10	3.0251E-10	3.5293E-10	4.0335E-10
Methanol	0.5222	9.7404E-11	1.4611E-10	1.9481E-10	2.4351E-10	2.9221E-10	3.4091E-10	3.8962E-10

Table 5: Results of electronic transition flow for N3- ZnS devices system at Δ^{0}=0.27 (eV) *and* N_s=8.25×10^{17} m^{-3} *with* T=325 K .

solvent	$\Lambda_{\frac{N3}{ZnS}}(eV)$	Rate of Electronic Transfer cm^2/Sec						
		$\langle \hat{H}_{\frac{N3}{ZnS}} \rangle$ eV/ state						
		1×10^{-3}	1.5×10^{-3}	2×10^{-3}	2.5×10^{-3}	3×10^{-3}	3.5×10^{-3}	4×10^{-3}
Morpholine	0.3167	4.0899E-10	6.1349E-10	8.1798E-10	1.0225E-09	1.2270E-09	1.4315E-09	1.6360E-09
Acetic acid	0.3361	3.7580E-10	5.6370E-10	7.5160E-10	9.3950E-10	1.1274E-09	1.3153E-09	1.5032E-09
1,2-Dim ethoxyethane	0.3582	3.3681E-10	5.0522E-10	6.7362E-10	8.4203E-10	1.0104E-09	1.1788E-09	1.3472E-09
Butanol	0.4441	1.9970E-10	2.9956E-10	3.9941E-10	4.9926E-10	5.9911E-10	6.9896E-10	7.9882E-10
Propanol-1	0.4621	1.7651E-10	2.6476E-10	3.5301E-10	4.4126E-10	5.2952E-10	6.1777E-10	7.0602E-10
Ethanol	0.4871	1.4793E-10	2.2189E-10	2.9585E-10	3.6982E-10	4.4378E-10	5.1774E-10	5.9171E-10
Propionitrile	0.4904	1.4442E-10	2.1663E-10	2.8883E-10	3.6104E-10	4.3325E-10	5.0546E-10	5.7767E-10
Acetonitrile	0.5176	1.1824E-10	1.7735E-10	2.3647E-10	2.9559E-10	3.5471E-10	4.1383E-10	4.7294E-10
Methanol	0.5222	1.1426E-10	1.7140E-10	2.2853E-10	2.8566E-10	3.4279E-10	3.9992E-10	4.5705E-10

Table 6:Results of electronic transition flow for N3- ZnS devices system at $\Delta^0 = 0.27\ (eV)$ and $N_s = 1.4 \times 10^{20} m^{-3}$ with $T = 320\ K$.

solvent	$\Lambda_{\frac{N3}{ZnS}}(eV)$	**Rate of Electronic Transfer** cm²/ Sec $\langle \hat{H}_{\frac{N3}{ZnS}} \rangle$ **eV/ state**						
		1×10^{-3}	1.5×10^{-3}	2×10^{-3}	2.5×10^{-3}	3×10^{-3}	3.5×10^{-3}	4×10^{-3}
Morpholine	0.3167	6.0119E-08	9.0178E-08	1.2024E-07	1.5030E-07	1.8036E-07	2.1042E-07	2.4048E-07
Acetic acid	0.3361	5.5193E-08	8.2789E-08	1.1039E-07	1.3798E-07	1.6558E-07	1.9318E-07	2.2077E-07
1,2-Dim ethoxyethane	0.3582	4.9406E-08	7.4110E-08	9.8813E-08	1.2352E-07	1.4822E-07	1.7292E-07	1.9763E-07
Butanol	0.4441	2.9105E-08	4.3658E-08	5.8210E-08	7.2763E-08	8.7315E-08	1.0187E-07	1.1642E-07
Propanol-1	0.4621	2.5683E-08	3.8524E-08	5.1365E-08	6.4206E-08	7.7048E-08	8.9889E-08	1.0273E-07
Ethanol	0.4871	2.1474E-08	3.2210E-08	4.2947E-08	5.3684E-08	6.4421E-08	7.5158E-08	8.5895E-08
Propionitrile	0.4904	2.0957E-08	3.1436E-08	4.1915E-08	5.2394E-08	6.2872E-08	7.3351E-08	8.3830E-08
Acetonitrile	0.5176	1.7112E-08	2.5668E-08	3.4224E-08	4.2780E-08	5.1336E-08	5.9892E-08	6.8447E-08
Methanol	0.5222	1.6529E-08	2.4794E-08	3.3058E-08	4.1323E-08	4.9588E-08	5.7852E-08	6.6117E-08

Table 7 : Results of electronic transition flow for N3- ZnS devices system at $\Delta^0 = 0.27\ (eV)$ and $N_s = 1.4 \times 10^{20} m^{-3}$ with $T = 325\ K$.

solvent	$\Lambda_{\frac{N3}{ZnS}}(eV)$	Rate of Electronic Transfer cm^2/Sec						
		$\langle \hat{H}_{\frac{N3}{ZnS}} \rangle$ eV/ state						
		1×10^{-3}	1.5×10^{-3}	2×10^{-3}	2.5×10^{-3}	3×10^{-3}	3.5×10^{-3}	4×10^{-3}
Morpholine	0.3167	6.9404E-08	1.0411E-07	1.3881E-07	1.7351E-07	2.0821E-07	2.4292E-07	2.7762E-07
Acetic acid	0.3361	6.3772E-08	9.5658E-08	1.2754E-07	1.5943E-07	1.9132E-07	2.2320E-07	2.5509E-07
1,2-Dim ethoxyethane	0.3582	5.7156E-08	8.5733E-08	1.1431E-07	1.4289E-07	1.7147E-07	2.0004E-07	2.2862E-07
Butanol	0.4441	3.3889E-08	5.0834E-08	6.7778E-08	8.4723E-08	1.0167E-07	1.1861E-07	1.3556E-07
Propanol-1	0.4621	2.9952E-08	4.4929E-08	5.9905E-08	7.4881E-08	8.9857E-08	1.0483E-07	1.1981E-07
Ethanol	0.4871	2.5103E-08	3.7654E-08	5.0205E-08	6.2757E-08	7.5308E-08	8.7859E-08	1.0041E-07
Propionitrile	0.4904	2.4507E-08	3.6761E-08	4.9014E-08	6.1268E-08	7.3521E-08	8.5775E-08	9.8029E-08
Acetonitrile	0.5176	2.0064E-08	3.0096E-08	4.0129E-08	5.0161E-08	6.0193E-08	7.0225E-08	8.0257E-08
Methanol	0.5222	1.9390E-08	2.9085E-08	3.8780E-08	4.8475E-08	5.8170E-08	6.7866E-08	7.7561E-08

The results in Table 3 indicated that the transition energy is affected by the dielectric constant and refractive index of the solvents used in the system, the transition energy at the contact area of N3-ZnS with solvents increases as the refractive index decreases, and the dielectric constant increases. In general, the type of solvent showed a strong effect on the N3 dye used in the solar cell, the interactions between the N3 dye and zinc sulfate, and the overall charge transfer dynamics. A solvent with good polarity and favorable interaction with N3 dye and ZnS can improve the efficiency of charge injection and reduce recombination losses such that Morpholine solvent. In turn, solvents that stabilize charge-separated states can enhance charge transfer efficiency.

According to the results obtained in Table 3 for the N3-ZnS system, the transition energy of the methanol solvent was higher than the other solvents used (0.522), and the morpholine solvent had the lowest transition energy (0.316).

N3-ZnS devices with the morpholine solvent have a low transition energy, which means an increase in the electronic transport rate, as the transport rate increases as the transition energy decreases.

According to the definition of transition energy, the energy difference between the excited state of N3 dye and the conduction band of ZnS needs to be renormalized. The results of the transition energy directly affect the efficiency of electron injection from the excited N3 dye to ZnS. A smaller difference between the excited state of N3 dye and the conduction band of ZnS allows for more efficient charge transfer. If the transition energy is too large (methanol 0.52224), the electron rate is lower 9.7404E-11 to 3.8962E-10 at 320 K, 1.1426E-10 to 4.5705E-10 at 325 K and 1.9390E-08 to 7.7561E-08 at 330 K, and the filament injection may be less efficient, which reduces the overall performance of the solar cell. The coupling strength refers to the interaction between the energy levels of the N3 dye and ZnS**.** The electron transfer rate values for the N3-ZnS system are shown in Tables (4), (5), (6), and (7). As expected, the electron transfer rate increases as the coupling strength increases and the transition energy decreases. A strong coupling allows the

charge to be transferred more efficiently from the N3 dye to the ZnS and vice versa. On the other hand, a weak coupling strength makes the charge transfer rate decrease, resulting in a lower solar cell efficiency. Improving the interaction between the dye and the semiconductor can significantly improve the charge injection and overall device performance.

In Tables (4) and (5), the highest electron transfer rate in the system was observed with the morpholine solvent ($1.417x\ 10^{-9}$) at the coupling strength ($4x10^{-3}$) compared to methanol which reached the lowest electron transfer rate (3.8962E-10) at the coupling strength ($4x10^{-3}$) at temperature 320 K, carrier concentration $N_s=8.25\times10^{17}\ m^{-3}$ and effective driving energy $\Delta^0=0.27$ (eV) When increasing the temperature to 325 K, an increase in electron transfer rate was observed for all solvents and the electron transfer rate was highest with the morpholine solvent (1.6360E-09) at the coupling strength ($4x\ 10^{-3}$). Temperature affects the charge transfer rate due to its effect on the kinetic energy of charge carriers. For Tables(6) and (7) for temperatures 320 K and 325 K and charge carrier concentration $N_s=1.4\times10^{20}\ m^{-3}$ and effective driving energy $\Delta^0=0.27$ (eV), it was found that when the temperature is increased and the charge carrier concentration is increased and when the coupling strength is increased and the transition energy is decreased, the electronic transport rate increases, and the morpholine solvent had the highest rate at temperature 320K (2.4048E-07) and at temperature 325K (2.7762E-07) at the coupling strength ($4x\ 10^{-3}$). The lowest electron transfer rate was obtained with the methanol solvent at temperature 320K (6.6117E-08) and at temperature 325K (7.7561E-08) at the coupling strength ($4x10^{-3}$). At temperatures of 330 K, charge carriers become more energetic, which results in an increased charge transfer rate from the N3 dye to the zinc sulfate. Temperature can also increase recombination rates, which can hinder the overall charge transfer efficiency. The optimum temperature range is important to achieve a balance between rapid electron injection and reduced recombination. Based on the results obtained, the electron transfer rate was higher at 325 K temperature ,and charge carrier concentration $N_s=1.4\times10^{20}\ m^{-3}$ for the

morpholine solvent compared to the electron transfer rate of the system at 325 K temperature and charge carrier concentration N_s=8.25×10^{17} m^{-3} for the same solvent.

The effect of charge carrier concentration is to increase the charge transport in the system. Tables (6) (7) indicate that higher concentrations can enhance current generation by increasing the number of charge carriers available for transport. Furthermore, too high a concentration can lead to increased recombination, where charge carriers combine before they are collected, reducing the efficiency of the solar cell.

This study was provided valuable insights into the electronic properties of the N3-ZnS system, particularly in terms of the electro transfer rate, which is influenced by factors like charge carrier concentration, temperature, and solvent choice. The results highlight the role of electronic interactions between the donor (N3 dye) and acceptor (ZnS), demonstrating how these interactions govern the efficiency of charge transfer and the overall performance of dye-sensitized solar cells

However, the theoretical calculations presented provide valuable insights into the charge transport dynamics in the N3-ZnS heterojunction, and experimental validation is necessary to fully confirm the predictions. Future studies that include charge transport measurements in real DSSC devices, along with experimental data on the effect of charge carrier concentration and solvent selection, will be crucial to confirm the results. These results, once validated, could greatly enhance the design and optimization of dye-sensitized solar cells, providing potential improvements in efficiency and stability for practical applications in renewable energy technologies.

4. Conclusions

Based on the electron density of states and continuous energy levels, the N3-ZnS system was calculated and studied using quantum transport theory. The results showed that the transition energy is influenced by the electrical properties of the N3-ZnS heterojunction interface. The electron transfer rate of N3-ZnS is more affected by changes in system transition energy, temperature, electronic coupling strength, and charge carrier concentration than

at the same solvent concentration. Increasing the temperature increases the average movement of electrons from donor to acceptor as the temperature helps the electrons overcome the activation energy barrier. Increasing the concentration of charge carriers in a semiconductor directly affects the rate of electron transport since conductivity is directly proportional to the density of charge carriers, so increasing conductivity with increasing charge carrier concentration means that electrons can move more freely in the material, which contributes to increasing the transport coefficient in the system. The N3-ZnS device containing morpholine solvent and charge carrier concentration N_s=1.4×10^{20} m^{-3} showed much higher efficiency in electron transfer rate compared to the N3-ZnS device with charge carrier concentration N_s=8.25×10^{17} m^{-3} and the same solvent.

References

1. R. Sasikumar, S. Thirumalaisamy, B. Kim, and B. Hwang, Renewable and Sustainable Energy Reviews ***199***, 114549, (Jul. 2024). DOI: 10.1016/J.RSER.2024.114549.

2. A. M. Oni, A. S. M. Mohsin, M. M. Rahman, and M. B. Hossain Bhuian, *Energy Reports* **11**, 3345–3366, (Jun. 2024). DOI: 10.1016/J.EGYR.2024.03.007.

3. S. Chen, L. Yang, J. Zhang, Y. Yuan, X. Dong, and P. Wang, *ACS Photonics* **4** (1), 165–173, (Jan. 2017). DOI: 10.1021/ACSPHOTONICS.6B00772/SUPPL_FILE/PH6B00772_SI_001.PDF.

4. L. He, Y. Guo, and L. Kloo, *Physical Chemistry Chemical Physics* **23** (48), 27171–27184, (Dec. 2021). DOI: 10.1039/D1CP02412D.

5. H. J. M. Al-Agealy, H. Hadi, D. Al-Hasan, R. Abdul, H. Muslim, and M. A. Hassooni, *Journal of Theoretical and Applied Physics (JTAP)*, (Jul. 2024). DOI: 10.57647/J.JTAP.2024.SI-AICIS23.18.

6. M. A. Hassooni and H. J. M. Al-Agealy, *Ibn Al-Haitham Journal For Pure and Applied Sciences* **23** (3), 2010.

7. N. Nahi, H. J. M. Al-Agealy, and H. M. Moghaddam, *Ibn AL-Haitham Journal For Pure and Applied Sciences* **37** (1), 187–197, (Jan. 2024). DOI: 10.30526/37.1.3235.

8. E. H. Rasheed and H. J. M. Al-Agealy, *AIP Conf Proc*

2769 (1), (Apr. 2023). DOI: 10.1063/5.0129535/2884810.

9. H. J. M. Al-Agealy et al., *J Phys Conf Ser* **1003** (1), 012122, (May 2018). DOI: 10.1088/1742-6596/1003/1/012122.

10. M. Grätzel, *Journal of Photochemistry and Photobiology C: Photochemistry Reviews* **4** (2), 145–153, (Oct. 2003). DOI: 10.1016/S1389-5567(03)00026-1.

11. H. J. M. Al-Agealy, M. A. H. Hassoni, M. S. Ahmad, R. I. Noori, and S. S. Jheil, *Ibn AL-Haitham Journal For Pure and Applied Science* **27** (1), 176–187, 2017.

12. A. Kipkorir and P. V. Kamat, *Journal of Chemical Physics* **156** (17), (May 2022). DOI: 10.1063/5.0090875/2841278.

13. M. Okutan, F. Yakuphanoğlu, M. I. Okutan, A. Bablich, and P. Haring Bolívar, *Physica B Condens Matter* **685**, 416027, (Jul. 2024). DOI: 10.1016/J.PHYSB.2024.416027.

14. S. N. F. Mohd-Nasir, M. Y. Sulaiman, N. Ahmad-Ludin, M. A. Ibrahim, K. Sopian, and M. A. Mat-Teridi, *International Journal of Photoenergy* **2014**, 370160, 2014. DOI: 10.1155/2014/370160.

15. M. Ben Manaa, N. Bouaziz, A. Ben Lamine, B. Schmaltz, N. Berton, and F. T. Van, *J Alloys Compd* **765**, 385–395, (Oct. 2018). DOI: 10.1016/J.JALLCOM.2018.06.234.

16. J. A. Salam, A. R, A. M. Anand, A. Raj, and R. Jayakrishnan, *Solar Energy Materials and Solar Cells* **282**, 113374, (Apr. 2025). DOI: 10.1016/J.SOLMAT.2024.113374.

17. R. Singh and R. R. Singh, 2022, Accessed: Sep. 15, 2024.

18. J. W. Norbury, *QUANTUM MECHANICS* (Book), University of Wisconsin-Milwaukee, Chapter 2, p44, 2000.

19. J. Garrison and R. Chiao, *Quantum optics*, OUP Oxford, 2008.

20. C. E. Burkhardt and J. J. Leventhal, *Foundations of Quantum Physics* **2008**, DOI: 10.1007/978-0-387-77652-1.

21. A. F. J. Levi, *Applied quantum mechanics*, Cambridge University Press, 2023.

22. T. S. Al Maadhede, M. H. Jumali, H. J. M. Al-Agealy, C. C. Yap, A. D. Ayada, and A. H. Shaban, *Energy Reports* **9**, 427–434, (Sep. 2023). DOI: 10.1016/J.EGYR.2023.05.247.

23. H. M. Obeed and H. J. M. Al-

Agealy, *IOP Conf Ser Mater Sci Eng* **871** (1), 012093, (Jun. 2020). DOI: 10.1088/1757-899X/871/1/012093.

24. A. K. Saadon and H. J. M. Al-agealy, *Energy Reports* **6**, 28–35, (Feb. 2020). DOI: 10.1016/J.EGYR.2019.10.015.

25. M. A. Hassooni and H. J. M. Al-Agealy, *Ibn Al-Haitham Journal For Pure and Applied Sciences* **24** (3), 2011.

26. M. K. Nazeeruddin et al., *J Am Chem Soc* **115** (14), 6382–6390, (Jul. 1993). DOI: 10.1021/JA00067A063/ASSET/JA00067A063.FP.PNG_V03.

27. Y. R. Farah and A. T. Krummel, *Journal of Chemical Physics* **157** (4), (Jul. 2022). DOI: 10.1063/5.0099543/16547494/044702_1_ACCEPTED_MANUSCRIPT.PDF.

28. M. J. Weber, *Handbook of Optical Materials* (Handbook of Optical Materials), (Oct. 2018). DOI: 10.1201/9781315219615.

29. P. Patnaik, *Handbook of inorganic chemicals*, **529**, McGraw-Hill New York, 2003.

30. I. Smallwood, *Handbook of organic solvent properties*, Butterworth-Heinemann, 2012.

31. S. S. A. Shah et al., "Decreasing of Optical Bandgap and N/P-Type Charge Carriers Variations in Cu Doped Zns Thin Films for Buffer Layer Applications in Solar Cell Devices", DOI: 10.2139/SSRN.4349336.

32. N. S. Lewis, *Journal of Physical Chemistry B* **102** (25), 4843–4855, (Jun. 1998). DOI: 10.1021/JP9803586/ASSET/IMAGES/LARGE/JP9803586F00005.JPEG.

33. S. Hlynchuk, M. Lancaster, M. MacInnes, R. Vasquez, and S. Maldonado, *Springer Handbooks*, 767–804, 2022. DOI: 10.1007/978-3-030-63713-2_27.